Adipose-Derived Mesenchymal Stem Cells from the Elderly Exhibit Decreased Migration and Differentiation Abilities with Senescent Properties

Meichen Liu[1], Hua Lei[1], Ping Dong[1], Xin Fu[1], Zhigang Yang[1], Ying Yang[1], Jiguang Ma[1], Xia Liu[1], Yilin Cao[1], and Ran Xiao[1]

Abstract

Adipose-derived stem cells (ASCs) can be applied extensively in the clinic because they can be easily isolated and cause less donor-site morbidity; however, their application can be complicated by patient-specific factors, such as age and harvest site. In this study, we systematically evaluated the effects of age on the quantity and quality of human adipose-derived mesenchymal stem cells (hASCs) isolated from excised chest subcutaneous adipose tissue and investigated the underlying molecular mechanism. hASCs were isolated from donors of 3 different age-groups (i.e., child, young adult, and elderly). hASCs are available from individuals across all age-groups and maintain mesenchymal stem cell (MSC) characteristics. However, the increased age of the donors was found to have a significant negative effect on hASCs frequency base on colony-forming unit fibroblasts assay. Moreover, there is a decline in both stromal vascular fraction (SVF) cell yield and the proliferation rate of hASCs with increasing age, although this relationship is not significant. Aging increases cellular senescence, which is manifested as an increase in SA-β-gal-positive cells, increased mitochondrial-specific reactive oxygen species (ROS) production, and the expression of *p21* in the elderly. Further, advancing age was found to have a significant negative effect on the adipogenic and osteogenic differentiation potentials of hASCs, particularly at the early and mid-stages of induction, suggesting a slower response to the inducing factors of hASCs from elderly donors. Finally, impaired migration ability was also observed in the elderly group and was determined to be associated with decreased expression of chemokine receptors, such as *CXCR4* and *CXCR7*. Taken together, these results suggest that, while hASCs from different age populations are phenotypically similar, they present major differences at the functional level. When considering potential applications of hASCs in cell-based therapeutic strategies, the negative influence of age on hASC differentiation potential and migration abilities should be taken seriously.

Keywords

human adipose-derived mesenchymal stem cells (hASCs), aging, cell senescence, differentiation, migration

Introduction

Adipose tissue is an ideal source of mesenchymal stem cells (MSCs) because high amounts of adipose-derived MSCs (ASCs) with minimal invasiveness are easily accessible.[1] ASCs are stable over long-term culture, expand easily in vitro, and possess multilineage potential, differentiating into adipogenic, osteogenic, chondrogenic, and angiogenic cells. Nicpon et al. confirms the long-term beneficial influence resulting from ASC therapy in horse bone spavin treatment, in contrast to routine steroid usage.[2] ASCs also have been used as a cell therapy in several human clinical trials, including those on soft tissue augmentation, idiopathic pulmonary fibrosis,[3] and myocardial ischemia.[4]

[1] Research Center of Plastic Surgery Hospital, Chinese Academy of Medical Sciences and Peking Union Medical College, Beijing, People's Republic of China

Corresponding Authors:
Xia Liu, Yilin Cao, and Ran Xiao, Research Center of Plastic Surgery Hospital, Chinese Academy of Medical Sciences and Peking Union Medical College, Ba-Da-Chu Road 33, Beijing 100144, People's Republic of China.
Emails: liuxia@psh.pumc.edu.cn; yilincao@yahoo.com; xiaoran@psh.pumc.edu.cn

Aged patients are the most feasible candidates for the therapeutic use of stem cells. However, aging is believed to negatively impact tissue repair and healing.[5] Stem cell function generally declines with age. Several studies on ASCs have reported alterations in the number, proliferation, and differentiation potential of MSCs with respect to donor age using both animal and human models. Zhu et al. isolated ASCs from adipose tissue obtained from female patients undergoing liposuction aged between 20 and 58 years and found that ASCs obtained from older donors appeared to have a slower rate of proliferation.[6] Although adipogenic potential was determined to be unrelated to donor age, a distinct relationship between donor age and osteogenic potential has been observed.[6] Moreover, Efimenko et al. demonstrated that there were no discernible age-associated changes in MSC marker profiles or ASC differentiation potential among ASCs isolated from subcutaneous adipose tissue during various surgical procedures from patients aged 2 to 82 years.[7] It became apparent that there are substantial differences in cell yield and the characteristic performance of ASCs, which are dependent on the donor site, the processing method used, and tissue sampling errors.

Due to the availability of ASCs, the cells used in most studies are obtained from liposuction surgery; therefore, most subjects are between 20 and 60 years old (i.e., ASCs are restricted to individuals likely to undergo liposuction). However, less research has been done on children and individuals over 60 years old. In contrast, studies on individuals over a wide age span lack systematic and comprehensive analyses. Furthermore, the effects of age on the migration ability of ASCs are not well-understood. It is known that migration plays an important role in the therapeutic function of stem cells. ASCs can migrate toward the region of tissue injury, responding to high levels of chemokines at the site of tissue damage.

The aim of the current study was to systematically investigate the impact of aging on the properties of ASCs obtained from excised adipose tissue, including cell morphology, senescent properties, and adipogenic and osteogenic potential, with special emphasis on their migration ability. The obtained results provide new insights into the molecular mechanisms underlying the age-related decline of the therapeutic potential of stem cells.

Materials and Methods

Human Adipose Tissue Samples

This study was conducted in accordance with the ethics committee of Plastic Surgery Hospital (Institute), Chinese Academy of Medical Sciences and Peking Union Medical College. Written informed consent for the harvest and use of adipose tissue samples for research purposes was obtained from each patient.

Human subcutaneous adipose tissue samples (>5 mL) were excised from the right chest regions of both male and female donors during various surgical procedures. Samples were divided into the following 3 distinct age-groups

Table 1. Patient Characteristics.

Variables	Child Group	Young Adult Group	Elderly Group
No. of patients	10	8	6
Age, years	7.6 (6–12)	24.8 (22–27)	66.3 (60–73)
Gender, male, n (%)	6 (60%)	5 (62.5)	4 (66.7)
BMI (mean ± SEM; kg/m^2)	20.4 ± 0.5	20.7 ± 0.8	21.4 ± 0.5

Abbreviations: BMI, body mass index; SEM, standard error of mean.

(Table 1): child (6 to 12 years; $n = 10$; 6 males and 4 females), young adult (22 to 27 years; $n = 8$; 5 males and 3 females), and elderly (60 to 73 years; $n = 6$; 4 males and 2 females). Each tissue sample was processed simultaneously by both manual and automated methods for all comparative studies.

SVF Isolation and Viability Assay

The stromal vascular fraction (SVF) was isolated enzymatically from excised fat tissue by digestion with collagenase. Briefly, the fat tissue was washed 2 or 3 times with phosphate-buffered saline (PBS), finely minced, and digested with 0.1% (w/v) type 1 collagenase (Sigma-Aldrich, St Louis, MO, USA) at 37 °C for 60 min with gentle agitation. The suspension was filtered through a nylon mesh (100 mesh) followed by centrifugation at 1,000 rpm for 10 min, and the final pellet was resuspended in culture medium. The nucleated cells were harvested as the SVF.

SVF yield was calculated as the initial cell number immediately after digestion divided by the same volume of the specimens. Cell concentration and viability were assessed on a Muse Cell Analyzer using the Muse Cell Count and Viability Assay (Merck Millipore, Darmstadt, Germany).

Culture of Human Adipose-Derived Mesenchymal Stem Cells (hASCs) and MSC Characteristic Examination

Cells were plated at a density of 1.5×10^5 cells/cm^2 for culture in Mesenchymal Stem Cell Medium (MSCM, ScienCell, Carlsbad, CA, USA) containing 10% fetal bovine serum (FBS, HyClone, South, Logan, UT, USA) in a humidified 37 °C incubator with 5% CO$_2$. Forty-eight hours after isolation, unattached cells were washed off, and the medium was changed every 2 d. hASC morphology was evaluated under phase contrast microscopy during culture. At the third passage, the expression of MSC surface markers (CD44, CD73, CD90, and CD105) was analyzed using a Stemflow Human MSC Analysis Kit (BD Biosciences, San Jose, CA, USA) on a FACSAria II flow cytometer.

Colony-Forming Unit Fibroblasts (CFU-Fs), Cell Proliferation, Apoptosis, and Cell Cycle Assays

The clonogenic ability of hASCs from the different age donors was determined by a CFU-Fs assay, as described in

the literature.[8] Briefly, freshly prepared passage 1 hASCs were seeded at a density of 4 cells/cm^2 in 55 cm^2 dishes (Corning, Tewksbury, MA, USA). After 10 d, the plastic adherent colonies were stained with 1% crystal violet (Beyotime, Shanghai, China). Colonies with diameters greater than 1 mm were taken into account.

The number of viable cells was quantified by the CellTiter 96 AQueous One Solution Cell Proliferation kit (Promega, WI, USA) following the manufacturer's instructions. In brief, 20 μL of 3-[4, 5-dimethylthizol-2-yl]-5-[3 carboxymethoxyphynyl]-2-[4-sulfophenul]-2H-tetrazolium inner salt (MTS)-based assay was added in each well and incubated for 4 h at 37 °C. The absorbance was measured at 490 nm on a PerkinElmer EnSpire Multimode Plate Reader.

A Muse Cell Analyzer was used for apoptosis studies using the Muse Annexin V & Dead Cell Assay. Cells were harvested, washed with PBS, and incubated with annexin V binding buffer according to the manufacturer's instructions. The percentage of normal, apoptotic, and necrotic cells was analyzed with a Muse Cell Analyzer (Millipore, Billerica, MA, USA).

Approximately 1×10^6 cells were centrifuged and washed with PBS. Washed cells were fixed with 70% ethanol and incubated for 3 h at -20 °C. Approximately 200 μL of fixed cells and an equal volume of Muse cell cycle reagent were mixed and incubated for 30 min at room temperature in the dark. The cell cycle was analyzed using a Muse Cell Analyzer (Millipore).

The expression levels of *c-Jun, c-Fos, caspase8, Bcl-2*, and *CHEK1* genes were detected by real-time quantitative reverse transcription-polymerase chain reaction (qRT-PCR) (Roche, LightCycler 480, Switzerland).

Cellular Senescence Assay

Senescence-associated β-galactosidase (SA-β-gal) staining was performed using a β-galactosidase Staining Kit (Beyotime, Shanghai, China) according to the manufacturer's instructions. Briefly, 5×10^4 hASCs (passage 5) were seeded onto 6-well plates and incubated with freshly prepared β-gal staining solution overnight at 37 °C in the absence of CO$_2$. hASCs were washed with PBS, and the blue color (i.e., senescent cells) was observed under microscopy. Phase contrast images were taken, and the percentage of SA-β-gal-positive cells was calculated by dividing the number of blue cells by the total number of cells, multiplied by 100.

Mitochondrial superoxide content was evaluated using MitoSOX Red reagent (Invitrogen, NY, USA) following the manufacturer's instructions. Passage 2 hASCs were cultured on glass chamber slides and incubated with 1 mL of 5 μM MitoSOX reagent working solution for 10 min at 37 °C, protected from light. Nuclei were stained with diamidino-2-phenylindole (DAPI) and imaged by fluorescence microscopy (Leica, Wetzlar, Germany).

2,7-Dichlorodi-hydrofluorescein diacetate (DCFH-DA) (Invitrogen) was used to measure total cellular reactive oxygen species (ROS) according to the manufacturer's instructions.

hASCs (5×10^5) were incubated with 7 μM DCFH-DA working solution for 5 min at 37 °C. Cells were then harvested and immediately evaluated on a flow cytometer (BD).

Proteasome activity was determined using the proteasome activity assay kit (Abcam, Cambridge, MA, USA) following the manufacturer's instructions. Briefly, cells were incubated with specific luminogenic proteasome substrates, Suc-Leu-Leu-Val-Tyr-7-amino-4-methylcoumarin (Succ-LLVY-AMC), and the free AMC fluorescence was measured on a fluorometric microplate reader at 350 of the 440 nm.

The expression levels of human telomerase reverse transcriptase (*hTERT*) and histone deacetylase (*SIRT1*), *p53, p21, p16*, and *RB1, RB2* genes were detected by qRT-PCR.

Adipogenic and Osteogenic Differentiation Potential Assay

hASCs were seeded at a density of 7.5×10^4 cells/mL onto 6-well plates (Corning, Tewksbury, MA, USA) and cultured until 90% confluence before switching to adipogenic medium (AM: growth medium supplemented with 2 nM dexamethasone, 33 μM biotin, 17 μM pantothenic acid, 0.5 mM isobutylmethylxanthine, 5 μM rosiglitazone, and 1 μM insulin; all from Sigma-Aldrich). After 4, 8, and 12 d in AM, adipogenesis was assessed by the qRT-PCR analysis of differentiation markers, including peroxisome proliferator-activated receptor (*PPAR-γ*), Ccaat enhancer binding protein-α (*CEBP-α*), fatty acid binding protein 4 (*FABP-4*), and adiponectin; key enzyme genes involved in lipid metabolism, including lipoprotein lipase (*LPL*), glycerol-3-phosphate dehydrogenase (*GPDH*), fatty acid synthase (*FASN*), acetyl-CoA carboxylase alpha (*ACC1*), and lipase hormone sensitive (*HSL*), and energy metabolism-related genes, including *PPAR-γ*, coactivator 1 alpha (*PGC1*), and uncoupling protein 1 (*UCP1*). Triglyceride content in differentiated cells was identified using 0.3% Oil Red O (Sigma-Aldrich). Cell images were collected using inverted microscopy. Stained oil droplets were dissolved in isopropyl alcohol and measured by reading the absorbance at 510 nm on a microplate reader (Thermo Scientific, NanoDrop 2000C, BD Biosciences, San Jose, CA, USA).

To induce osteogenic differentiation, cells were seeded at a density of 5×10^4/mL onto 6-well plates. After reaching 80% confluence, osteogenic differentiation was induced by replacing the medium with osteogenic medium (OM: growth medium supplemented with 0.1 μM dexamethasone, 0.05 mM ascorbic acid (AA), and 10 mM sodium glycerophosphate; all from Sigma-Aldrich). To assess osteogenic differentiation, RNA was isolated after induction for 7, 14, and 21 d. The messenger RNA (mRNA) expression of differentiation markers (i.e., *Runx-2*, alkaline phosphatase [*ALP*], osteocalcin [*OCN*], osteopontin [*OPN*], and bone morphogenetic protein 2 [*BMP2*]) was then determined by qRT-PCR. The accumulation of calcium deposits was visualized by staining with Alizarin Red S dye and quantified by colorimetric analysis at 562 nm.

hASC Migration Ability Assay

A scratch test and a transwell assay were used to determine the change in the migration ability of hASCs with age.

Briefly, hASCs were cultured on 6-well plates until reaching 90% confluence. The original medium was removed, and cells were washed with PBS. Cell scratches were made with a 200-µL pipette tip, and residual cells were washed away by PBS. Dulbecco's modified eagle's medium (DMEM) culture medium containing 2% FBS was used to culture cells for 24 h. Inverted microscopy was utilized to observe the healing condition of the cells after 6, 12, and 24 h. Transwell assays were performed using an 8-µm pore size transwell chamber (Corning) in 24-well plates. Cells were plated in the upper chamber of the transwell at a density of 2.5×10^4 cells/mL, while culture medium containing 10 µg/L stromal cell-derived factor 1 (SDF-1) was added in the lower chamber followed by incubation in a 5% CO_2 incubator at 37 °C. After incubation for 6 h, migrated cells appeared in the lower side of the transwell membrane and were fixed with 4% glutaraldehyde for 2 h and overnight with 2% Toluidine blue. The number of cells at the lower side was counted in 5 different randomly selected $10\times$ fields using bright-field microscopy.

The expression levels of chemokine receptors, such as *CXCR4* and *CXCR7* genes, were detected by qRT-PCR.

RNA Isolation and Real-Time Quantitative Reverse Transcription-Polymerase Chain Reaction (qRT-PCR)

Total RNA was extracted with TRIzol reagent (Invitrogen), and 1 µg was reverse-transcribed using Moloney murine leukemia virus (MMLV) Reverse Transcriptase (Invitrogen). qRT-PCR was performed using a Fast Synergy Brands (SYBR) Green Master Kit and a LightCycler 480 system (Roche) according to the manufacturer's instructions. The expression level of each target gene was normalized to 18S or β-actin and measured by the comparative Ct ($2^{-\Delta\Delta Ct}$) method. The specific oligonucleotide primer sequences are listed in Table 2.

Statistical Analysis

Experimental data were analyzed using GraphPad Prism 5 software (San Diego, CA, USA). Statistical significance was determined using one-way analysis of variance with Tukey's post hoc multiple comparison test for normally distributed data and otherwise by Kruskall–Wallis test. Data are expressed as the mean $\pm$ standard error of the mean. Values of $P < 0.05$ were considered statistically significant.

Results

Analysis of SVF Yield and Viability

The adipose-derived SVF is a heterogeneous population of cells including MSC-like cells, endothelial progenitor cells, and hematopoietic cells. The yields and viabilities of freshly

Table 2. Primer Sequences used for qRT-PCR.

Gene	Primer 5′-3′
ACC1	F: CTGGTTTGTGGAAGTGGAAGG
	R: CTGCGGATTTGCTTGAGGAC
Adiponectin	F: CTTCCGTCACCTCTAAATCC
	R: GTCATCCCTAACTTCAGTGG
ALP	F: GGCTCCAGGGATAAAGCAGGTC
	R: GCTCCAGGGCATATTTCAGTGTC
BCL2	F: AGATGGGAACACTGGTGGAG
	R: CTTCCCCAAAAGAAATGCAA
BMP-2	F: ACCCGCTGTCTTCTAGCGT
	R: TTTCAGGCCGAACATGCTGAG
Caspase-8	F: AACCTCGGGGATACTGTCTG
	R: CCTGTCCATCAGTGCCATAG
CEBP-α	F: AGGAACACGAAGCACGATCA
	R: ACAGAGGCCAGATACAAGTG
c-Fos	F: CTTCAACGCAGACTACGAGG
	R: GACCGTGGGAATGAAGTTGG
c-Jun	F: CCAACATGCTCAGGGAACAG
	R: CTCAAGTCTGTCTCTCTGTG
CHEK1	F: AGCGGTTGGTCAAAAGAATG
	R: CCCTTAGAAAGCCGGAAGTC
CXCR7	F: CCAGCAGCAGGAAGAAGATG
	R: GGGCAGTAGGTCTCATTGTTG
CXCR4	F: TCTTCCTGCCCACCATCTAC
	R: GCGTGATGACAAAGAGGAGG
FABP4	F: GAAAGTCAAGAGCACCATAACC
	R: GACGCATTCCACCACCAGTT
FASN	F: CCCACCTACGTACTGGCCTA
	R: TTGGCCTTGGGTGTGTACT
GPDH	F: TACAGCATCCTCCAGCACAA
	R: CCTGGAGATCCTGGTGACTA
hTERT	F:GGAGCAAGTTGCAAAGCATTG
	R: TCCCACGACGTAGTCCATGTT
HSL	F: GGAAGTGCTATCGTCTCTGG
	R: TCCTCACTGTCCTGTCCTTC
LPL	F: AGAGAGAGGACTTGGAGATG
	R: GGCTCTGACTTTATTGATCTC
OCN	F: CCTCACACTCCTCGCCCTAT
	R: TGGGTCTCTTCACTACCTCG
OPN	F: CAGCAACCGAAGTTTTCACTCCAG
	R: CACCATTCAACTCCTCGCTTTCC
PPAR-γ	F: TGGAATTAGATGACAGCGACTTGG
	R: CTGGAGCAGCTTGGCAAACA
PGC1α	F: TCCAGGTCAAGATCAAGGTC
	R: CGTGCTGATATTCCTCGTAG
p16	F: AACCTCGGGAAACTTAGATC
	R: TCTACGTTAAAAGGCAGGAC
p21	F: GCACTTTGATTAGCAGCGGA
	R: GAAAGACAACTACTCCCAGC
p53	F: TGCTCAAGACTGGCGCTAAA
	R: CAATCCAGGGAAGCGTGTCA
RB1	F: CCGTGTGCTCAAAAGAAGTG
	R: CCTTGTTTGAGGTATCCATGC
RB2	F: ACAGGTGCCAACAGTGACAT
	R: ATAGGGAGAGAGTGGAGGA
RUNX2	F: ACTGGCGCTGCAACAAGAC
	R: CCCGCCATGACAGTAACCA
SIRT1	F: TAATAGAGTGGCAAAGGAGCAG
	R: TACTGCCACAAGAACTAGAGGA
UCP1	F: GTTTAGGAAGCAAGATTTTAGC
	R: GTACAATTGATGATGACACTTC

isolated cell populations were quantified to determine how age influences the cell availability within tissue sources and survival after isolation. The number of total nucleated cells was $7.28 \times 10^5 \pm 5.52 \times 10^4$/mL with $82.0 \pm 3.45\%$ cell viability in the child group, $6.32 \times 10^6 \pm 4.51 \times 10^4$/mL with $80.0 \pm 1.34\%$ cell viability in the young adult group, and $5.53 \times 10^5 \pm 9.9 \times 10^4$/mL with $80.9 \pm 4.43\%$ cell viability in the elderly group (Fig. 1A and B). The mean cell yield and viability values obtained in the present study are consistent with those from previously published reports.[9] However, we were unable to demonstrate a significant difference between the different age-groups, although there was a trend indicating that the SVF cell yield decreases with increasing donor age.

hASCs from Donors of Different Ages Maintain MSC Characteristics

As previously described, the SVF from the same volume of fat was plated and adherent colonies formed in all 3 groups after 24 h. hASCs were cultured to the third passage. The cells in all groups exhibited a fibroblast-like morphology, and there was no difference during passaging (Fig. 1C).

The surface protein expression of hASCs at passage 3 was examined by flow cytometry. The cells fulfilled all minimal criteria for defining MSCs according to the International Society for Cellular Therapy position statement[10]; they were positive (>95%) for CD44, CD73, CD90, and CD105 and had low expression (<5%) of negative markers (CD34, CD11b, CD19, CD45, and HLA-DR; Fig. 1D). There was no significant difference between groups regarding cell morphology and MSC marker expression.

hASCs from Elderly Donors Exhibit Senescent Properties

Age-dependent stem cell dysfunction can manifest in many forms, such as the loss of self-renewal and/or differentiation, increased apoptosis and senescence.

The amount of progenitor cells in SVF cells was assessed by the number of CFU-Fs. Increased age of the donor was found to have a significant negative effect on the hASC frequency (Fig. 2A). Nearly a 70% reduction in median CFU-Fs was noted in samples obtained from elderly group relative to those harvested from the child group.

Cell growth kinetics revealed a slight trend toward decreasing proliferation potential with age (Fig. 2B). However, no statistical significance was observed upon analysis. Consistent with these results, a decreasing trend of *c-Jun* and *c-Fos* gene expression, the key proto-oncogenes related to proliferation, with age was observed (Fig. 2C).

Apoptosis and its related genes, *caspase-8* and *Bcl-2*, did not appear to be significantly affected by donor age (Fig. 2D and E).

The cell cycle distribution of hASCs was determined using a Muse Cell Cycle Assay Kit. An assessment of the percentage of cells in G0/G1, S, and G2/M phase among the hASCs indicated a significant decrease in the number of cells in S phase. A slight increase in the number of cells in G0/G1 and G2/M in the elderly group compared with the other 2 groups was also observed (Fig. 2F). The expression of *CHEK1* (promotes a G2/M phase arrest), which plays a crucial role in the control of the cell cycle, was upregulated with increasing age, although the difference was not significant (Fig. 2G).

SA-β-gal activity is the most commonly used biomarker for the identification of senescent cells. We observed a significant increase in SA-β-gal-positive cells in passage 5 cells in the elderly group ($0.83 \pm 0.33\%$; $P < 0.05$) compared to the child group ($0.10 \pm 0.10\%$; Fig. 3A and B), although there was no significant difference in passage 3 hASCs between the different age-groups (data not shown). This result suggests that hASCs from elderly individuals are more susceptible to replicative senescence during in vitro amplification.

Aging is often associated with several cellular hallmarks of senescence, such as mitochondrial dysfunction, impaired proteasome activity, attenuated telomerase activity, epigenetic changes, and metabolic alterations.[11,12]

The mitochondria is a major source of intrinsic ROS production, and mitochondrial ROS are believed to be associated with aging.[13] A DCFH-DA assay showed an increase in total intracellular ROS production with increasing age (Fig. 3C and 3D), and MitoSOX Red staining demonstrated that mitochondrial-specific ROS production was increased in the elderly group (Fig. 3E).

The impaired proteasome activity is another important aspect of cellular senescence. As shown in Fig. 3F, proteasome activity displayed a rapid decrease in the child group compared to the young adult group, which did not, however, reach significance. The interindividual variation was the highest in the young adult group. The proteasome activity in elderly group was comparable to the young adult group.

Although decreased expression of *SIRT1* and *hTERT* with increasing age was evidenced by qRT-PCR, the differences between groups were statistically insignificant (Fig. 3G). The senescence markers *p53*, *p16*, and *p21* were also increased with increasing donor age, although the only significant difference was observed between the child group and the elderly group with respect to *p21* (Fig. 3H). The retinoblastoma family genes *RB1* and *RB2* also play major roles in controlling the cell cycle G1/S transition and in senescence.[14] As shown in Fig. 3H, although the mRNA expression of *RB1* decreased in an age-dependent manner, there was no significant difference between groups in *RB1* or *RB2* expression.

Adipogenic Differentiation Potential Decreases with Age Early, While the Overall Potential of hASCs to form Mature Adipocytes Is Comparable between Age Groups

To confirm adipogenesis, cells were stained with the lipid dye Oil Red O. Small lipid droplets were apparent in all 3
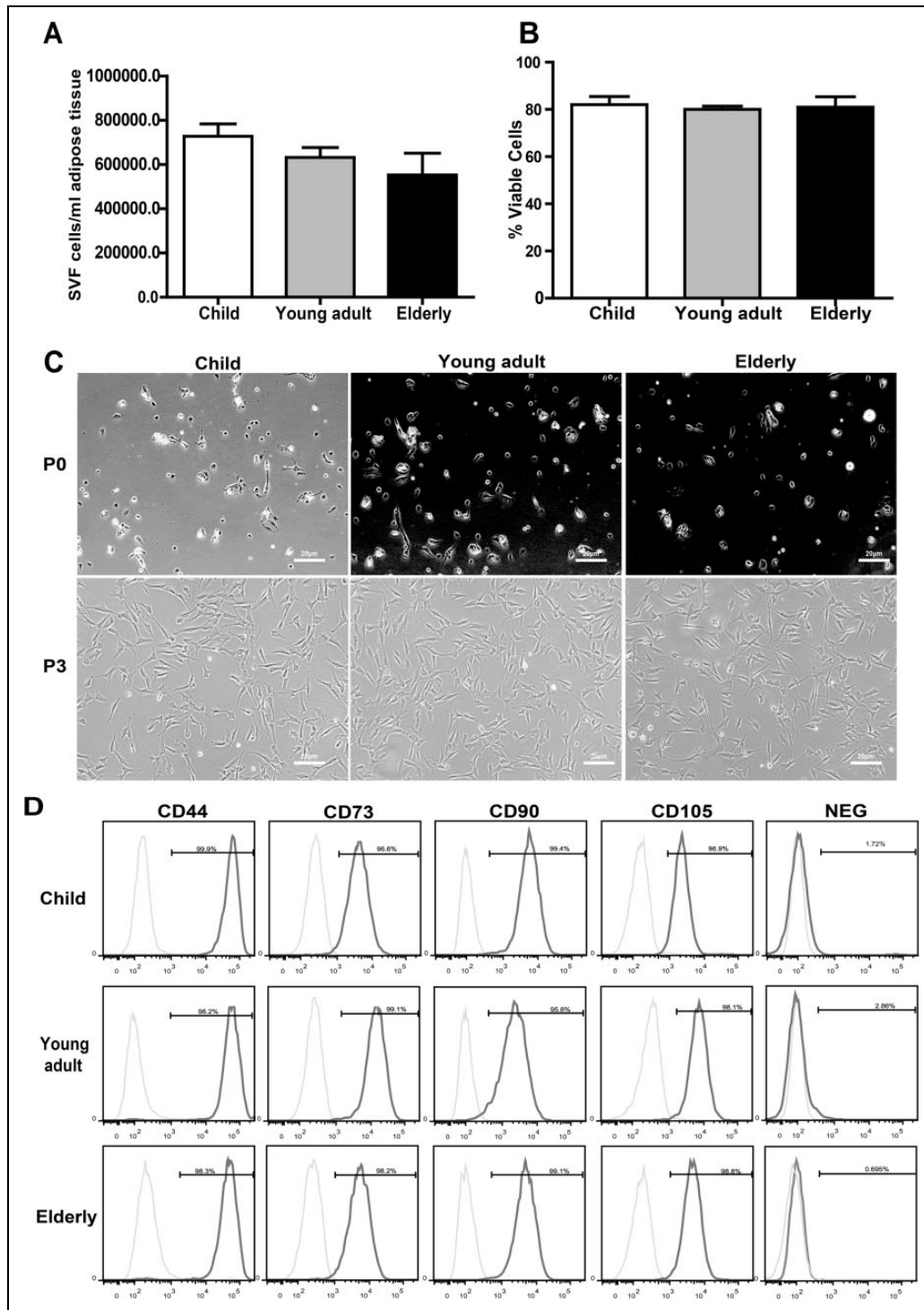
Fig. 1. Influence of age on stromal vascular fraction (SVF) yield, cell viability, and mesenchymal stem cell (MSC) characteristics. (A) A slight trend indicated that the SVF cell yield decreased with increasing donor age, but no significant difference was found between the different age-groups. (B) Donor age had no effect on human adipose-derived mesenchymal stem cells (hASCs) viability. (C) hASCs from different age-groups showed similar cellular morphologies at passage 0 and 3 (P0 and P3) under phase contrast microscopy (20X). (D) FACS analysis was used to determine the proportion of hASCs expressing MSC surface markers (CD44, CD73, CD90, and CD105). Experiments were carried out in triplicate. Data are expressed as the mean $\pm$ standard error of mean (SEM). FACS: fluorescent-activated cell sorting.

groups as early as 4 d following adipogenic induction and gradually increased with induction time. By 12 d of induction, large Oil Red O-positive lipid droplets had formed (Fig.

4A). The results of the semi-quantitative detection showed that the absorbance values between the 3 groups did not differ significantly at day 4, 8, or 12 (Fig. 4B).
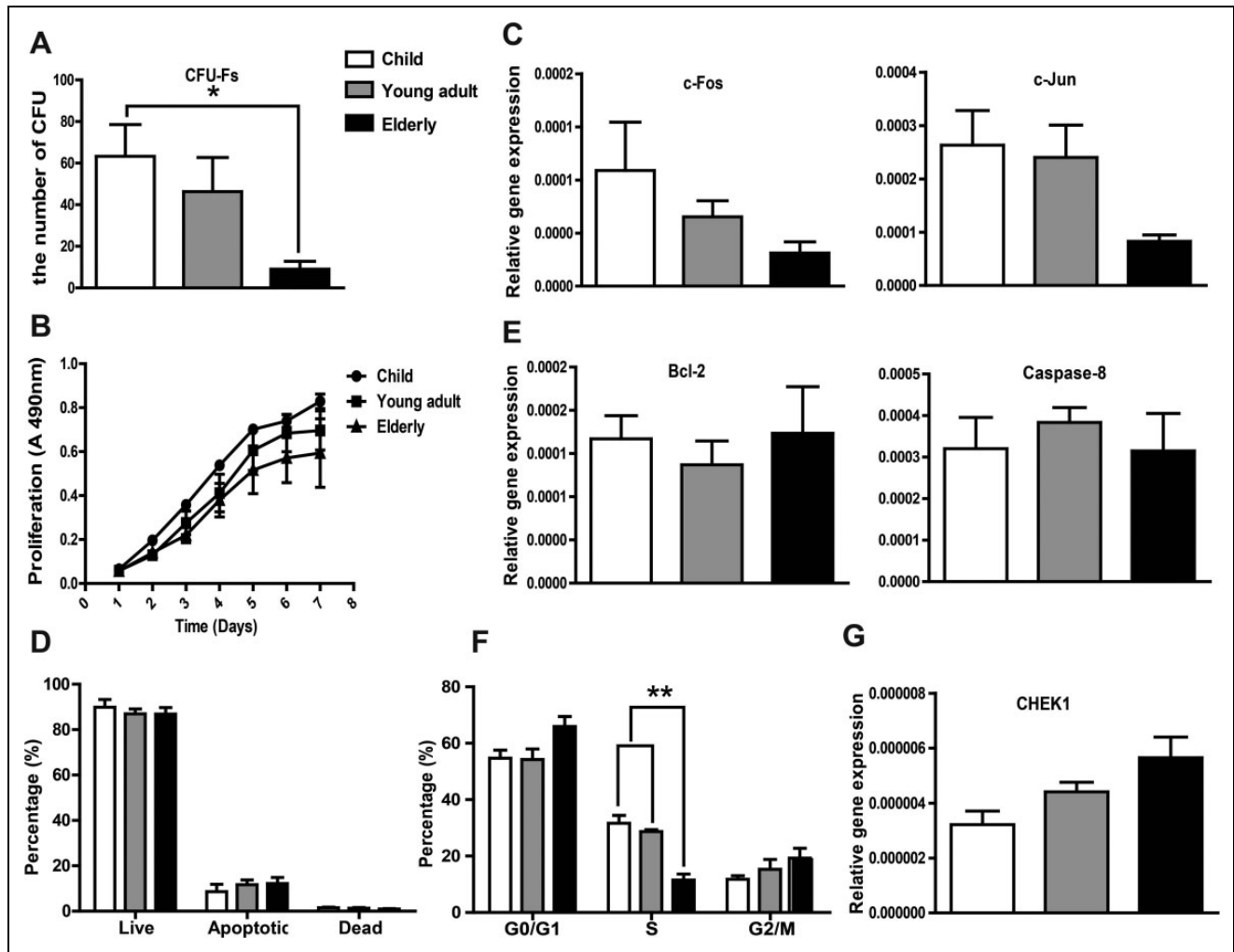
Fig. 2. Effect of donor age on human adipose-derived mesenchymal stem cells (hASCs) colony-forming unit fibroblasts (CFU-Fs), proliferation, apoptosis, and cell cycle distribution. (A) CFU-Fs assay showed the number of clone forming cells decreased significantly in elderly group compared with the child group. (B) Donor age had no effect on hASCs proliferation, as evidenced by the MTS assay. (C) qRT-PCR analysis of genes associated with proliferation (*c-Jun* and *c-Fos*) showing a decreasing trend with age. (D) Apoptosis was analyzed using a Muse Cell Analyzer, showing no significant difference between the different age-groups. (E) Expression of apoptosis-related genes *Bcl-2* and *caspase-8* were determined by qRT-PCR and did not appear to be significantly affected by donor age. (F) Cell cycle distribution of hASCs in different age-groups analyzed with a Muse Cell Analyzer. The number of cells in S phase in the elderly group was significantly decreased compared with the other 2 groups. (G) qRT-PCR analysis showed that the expression of *CHEK1*, a cell cycle-associated gene, was upregulated with increasing age, although the difference was not significant. Experiments were carried out in triplicate. Data are expressed as the mean $\pm$ standard error of mean [SEM]. *$P < 0.05$, **$P < 0.01$

To provide a more stringent and detailed quantitative measurement of adipogenesis, genes related to adipogenic differentiation (*PPAR-γ, CEBP-α, FABP4,* adiponectin, and *LPL*) and lipid synthesis (*GPDH, FASN, ACC1,* and *HSL*) were examined following induction at different times. As shown in Fig. 4C and D, *PPAR-γ, CEBP-α, FABP4*, and *LPL* were highly upregulated as early as 4 d induction in the child group, which differed significantly compared with the young adult and elderly groups. Lipid synthesis-related genes (*GPDH, FASN, ACC1,* and *HSL*) decreased with age during adipose induction (Fig. 4E). It is worth noting that there was a significant difference between the child group

and the other 2 groups with respect to *FASN* in hASCs without induction.

Consistent with the mRNA expression of adipogenic genes, low expression of thermogenic markers *UCP1* and *PGC1α* was found in the elderly group (Fig. 4F). Moreover, their response was slow when induced, suggesting that the adipose tissue lost brown-like features with aging.

Therefore, although their overall potential to form mature adipocytes was comparable, there were some variations during the early and mid-phases of adipogenic induction among the different age-groups. These results suggest that the response to the induction factors of hASCs is faster in children.
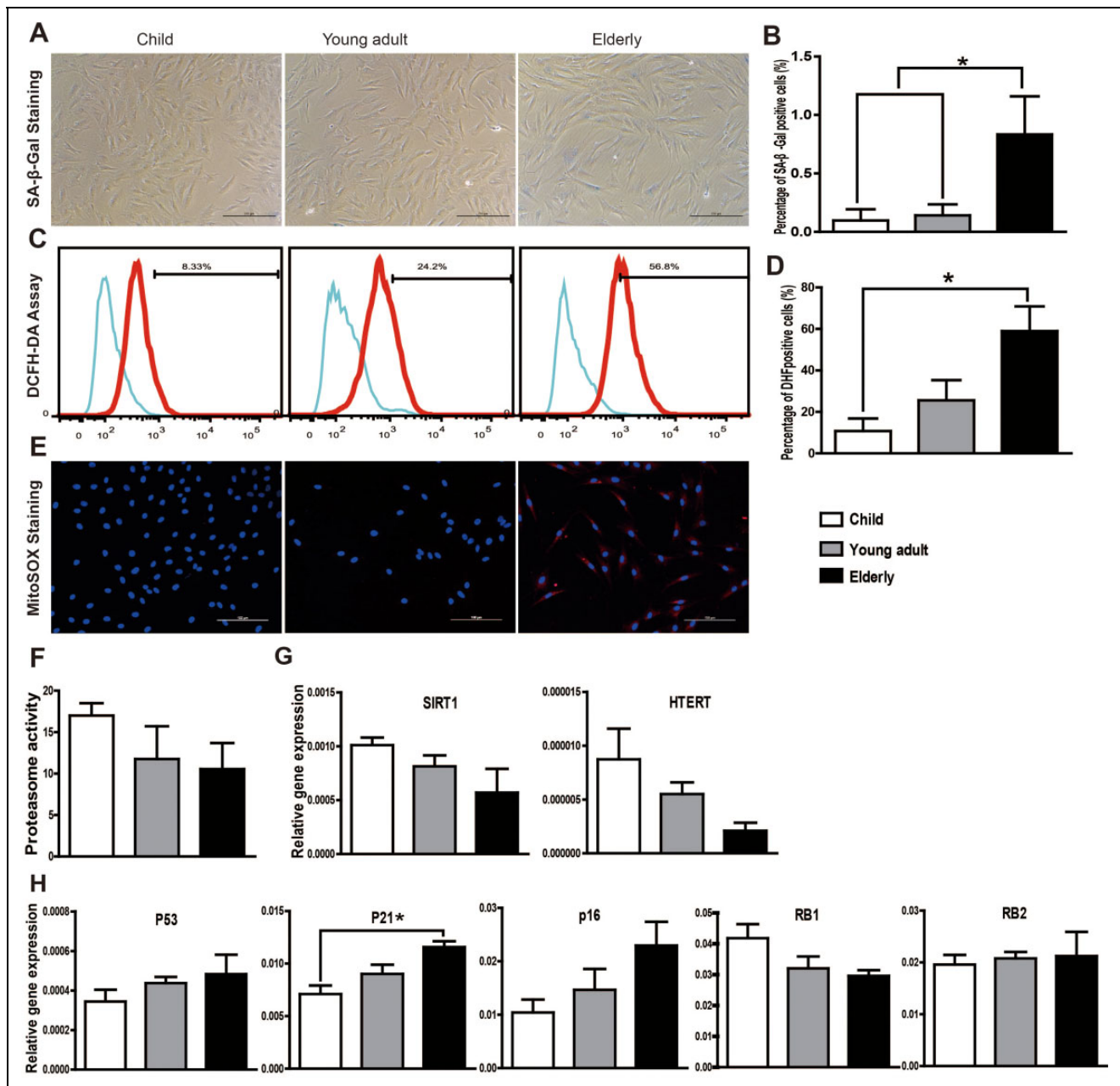
Fig. 3. Senescence state of human adipose-derived mesenchymal stem cells (hASCs) in different age-groups. (A) Representative pictures of senescence-associated β-galactosidase (SA-β-gal) staining (20× magnification). (B) The number of senescent cells (SA-β-gal-positive) was significantly higher in the elderly group. Positive cells were expressed as a percentage of total hASCs counted. (C) Total intracellular ROS production was measured using the DCFH-DA assay. (D) Quantitative analysis of the DCFH-DA assay revealed a significant increase in ROS production in the elderly group. (E) Representative pictures of MitoSOX Red staining demonstrating that mitochondrial-specific ROS production was increased in the elderly group. (F) Proteasome activity assay showed a decreasing trend with age increasing, although the difference was not significant. (G) Messenger RNA (mRNA) expression levels of *SIRT1* and *hTERT* were determined by qRT-PCR. Although there was no difference in their expression between the different age-groups, both exhibit a decreasing trend with increasing age. (H) qRT-PCR analysis showed that the mRNA expression levels of senescence markers *p53*, *p21*, and *p16* were increased with increasing donor age. The mRNA levels of *RB1* declined in an age-dependent manner, whereas the *RB2* expression level in 3 groups was comparable. Only *p21* mRNA expression showed significant difference between the child group and the elderly group. The expression of each gene was normalized to the amount of *GAPDH* RNA to calculate the relative amount of mRNA. All tests were performed in triplicate, and the data are expressed as the mean $\pm$ standard error of mean. *$P < 0.05$.
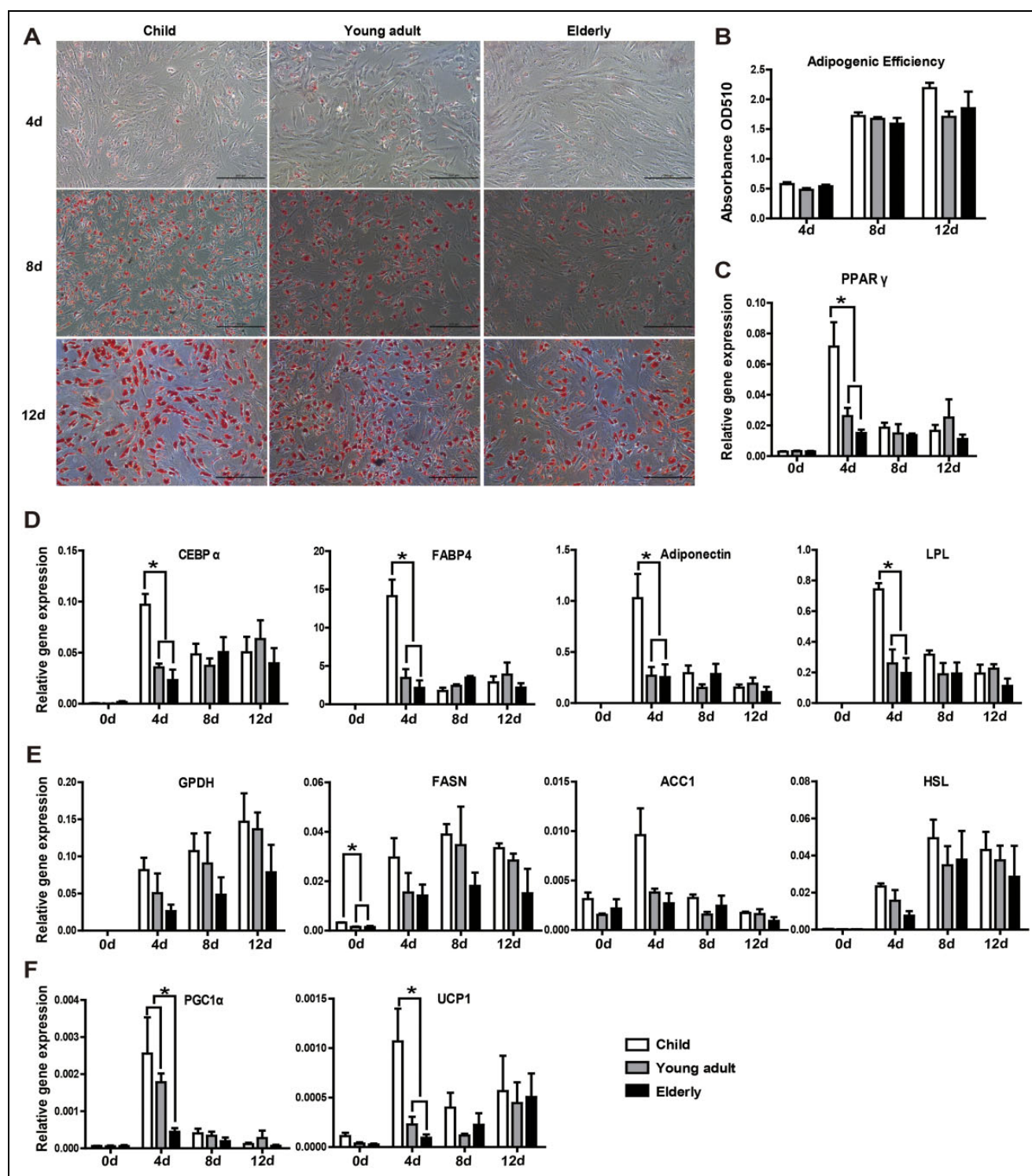
Fig. 4. Aging influences adipogenic differentiation potential at the early time of induction, while the overall potential to form mature adipocytes is comparable between age-groups. (A) Adipogenesis was confirmed in hASCs by Oil Red O staining. (B) Semi-quantitative detection by colorimetric evaluation of Oil Red O uptake showed no significant differences between the 3 groups. (C, D) Adipogenic differentiation was further confirmed through qRT-PCR analysis of genes related to adipogenic differentiation (*PPAR-γ, CEBP-α, FABP4,* adiponectin, and *LPL*). At the early time of induction (day 4), all genes related to adipogenic differentiation were significantly higher in the child group compared to the other 2 groups. (E) The expression of lipid synthesis-related genes (*GPDH, FASN, ACC1,* and *HSL*) in hASCs after adipogenic induction for 4, 8, and 12 d. There were no significant differences between the different age-groups. (F) The expression levels of thermogenic markers *UCP1* and *PGC1α* were significantly higher in the child group at the early induction stage. All tests were performed in triplicate, and the data are expressed as the mean $\pm$ standard error of mean (SEM). *$P < 0.05$.
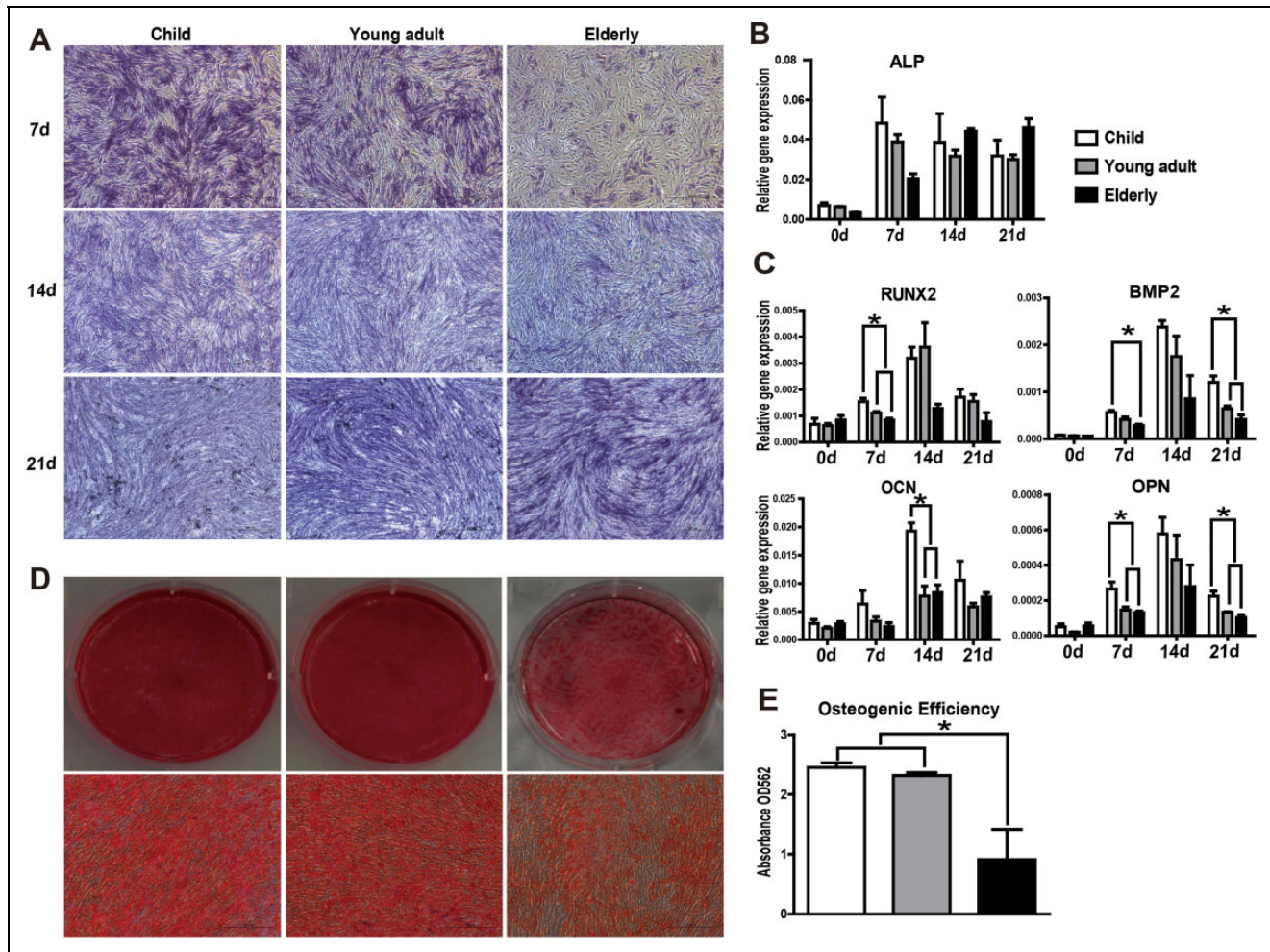
Fig. 5. Osteogenic differentiation diminishes with increasing age. (A) Representative pictures of alkaline phosphatase (ALP) staining (20× magnification). (B, C) Messenger RNA (mRNA) expression levels of osteogenic differentiation-related genes (*ALP, RUNX2, BMP2, OCN*, and *OPN*) were determined in human adipose-derived mesenchymal stem cells (hASCs) over the course of osteogenic differentiation by qRT-PCR. hASCs from aged donors had a diminished response to osteogenic inducers relative to that of young donors. (D) Alizarin Red S staining was used to visualize mineralization. Representative images were shown from 3 separate experiments. (E) Quantitative analysis of Alizarin Red S staining in hASCs cultures at day 14 after osteogenic induction revealed a significant decrease in matrix calcification in the elderly group compared to younger donors. All tests were performed in triplicate, and the data are expressed as the mean $\pm$ standard error of mean (SEM). *$P < 0.05$.

hASCs from Aged Patients Exhibit Impaired Osteogenic Potential

Osteogenesis was confirmed by ALP and Alizarin Red S staining. Increased ALP expression was observed in both the child and young adult groups during the early stages of osteogenesis and gradually decreased by days 14 and 21. In contrast, ALP expression gradually increased in the elderly group during osteogenic induction (Fig. 5A and B), suggesting that the response of hASCs from elderly donors to inducing factors is slower than those from the other groups.

To determine the factors involved in the osteogenic activity of hASCs, we analyzed the expression of various early-, mid-, and late-phase osteogenic differentiation markers, including *ALP, Runx2, BMP2, OPN*, and *OCN* by

qRT-PCR (Fig. 5C). Generally, these genes reached a maximum at day 14 and gradually decreased by day 21. The expression levels of *Runx2, BMP2*, and *OPN* were significantly higher in the child group compared to the other 2 groups at the early phase (day 7). *OCN* mRNA expression was significantly elevated in the child group compared to other 2 groups during the middle stage (day 14). By the late phase of differentiation at day 21, *BMP2* and *OPN* expression remained higher in the child group than in the other 2 groups. hASCs induced in OM for up to 21 d showed extensive mineralization in all 3 groups, as visualized by Alizarin Red S staining (Fig. 5D). Quantitative measurement of Alizarin Red S revealed a significant decrease in matrix calcification in the elderly group compared to the younger donors (Fig. 5E). Taken together, these data suggest a
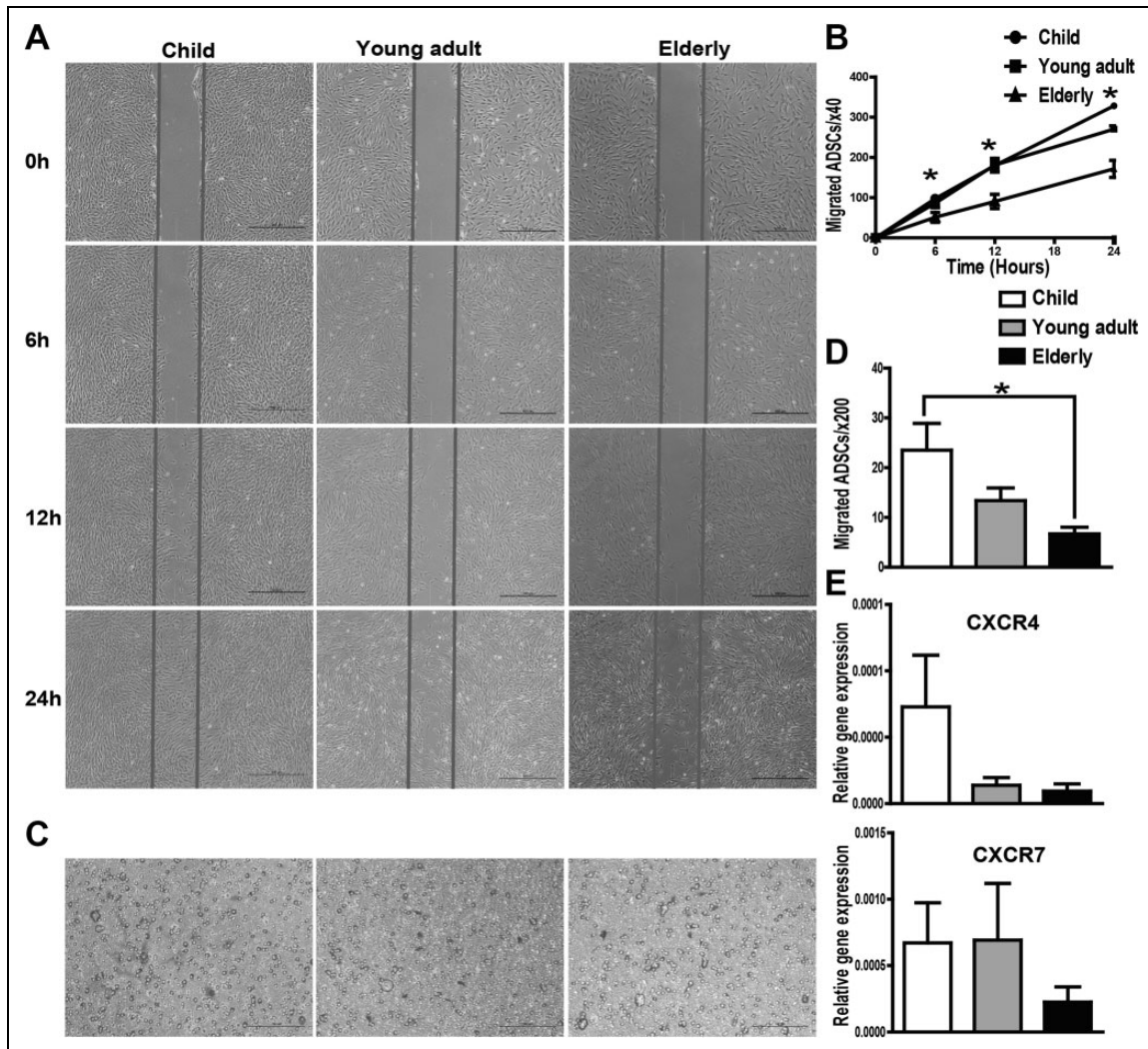
Fig. 6. Cell scratch test and transwell assay were used to examine the migration ability of human adipose-derived mesenchymal stem cells (hASCs). (A) Images from the scratch wound migration assay. Healing due to the cellular migration of hASCs was observed over a period of 6 and 24 h following scratch wounding. (B) Quantitative data from the cell scratch healing assay were shown. The migration ability of hASCs in the elderly group was decreased significantly at 6, 12, and 24 h compared to that of the child group. (C) Representative images of cell migration using a transwell assay. (D) Quantitative analysis of cell migration using the transwell assay. The number of migratory cells of the elderly group was reduced compared to that of the child group (within 6 h). (E) The messenger RNA (mRNA) expression levels of chemokine receptors *CXCR4* and *CXCR7* were decreased in the elderly group. All tests were performed in triplicate, and the data are expressed as the mean $\pm$ standard error of mean (SEM). *$P < 0.05$.

decrease in the osteogenic potential of hASCs isolated from elderly donors.

hASCs from Aged Patients Exhibit Impaired Migration Potential

The scratch test and transwell system were used to analyze the migration ability of hASCs. The results of the scratch test showed that the migration ability of hASCs was significantly decreased in the elderly group at 6, 12, and 24 h compared to that in the child group (Fig. 6A and B). Furthermore, the transwell assay revealed that the number of migratory cells of the elder group was reduced compared to that of the child group within 6 h (Fig. 6C and D). Therefore, we conclude that

the elderly derived ASCs show an impaired migration capability under basal conditions. To identify the pathway implicated in cell migration, we performed qRT-PCR to examine the expression of *CXCR4* and *CXCR7*. Consistent with the results of the migration assay, a significant reduction in *CXCR4* and *CXCR7* expression was observed in the elderly group compared with the younger groups (Fig. 6E), demonstrating that a decreased migration ability is associated with decreased expression of chemokine receptors in hASCs.

Discussion

hASCs are useful for cell therapy and have been used in several preclinical models of regeneration and clinical

trials.[15] The clinical applicability of hASCs spans all age-groups. Some studies have shown the effects of age on the proliferative and differentiation potentials of hASCs. However, the differences reported were found to depend on various factors, such as anatomic site, harvesting technique, donor gender, and body mass index.

In the present study, we investigated several distinct parameters, including the senescence, proliferation, and differentiation capacity together with the migration potential of hASCs derived from different age donor groups.

The fresh SVF of adipose tissue is a rich source of regenerative cells and is used for different clinical applications.[16] Cell yield, which reflects the total cell number obtained from the tissue (not only MSCs), and cell quality are the keys for maximizing the success of clinical studies. The results from the present study indicate a decreasing trend with increasing donor age, although there were no significant differences between groups. These findings are in agreement with existing data, suggesting that SVF yield and viability do not change significantly with donor age.[17] However, Dos-Anjos Vilaboa et al. showed a statistically significant decline in SVF cell yield with increasing age in female subjects[9] and that the postmenopausal status of patients could explain the reduced cell yield found in their study.

hASCs from different age donors were isolated and characterized in the study described herein. These cells consistently expressed the characteristic surface markers associated with MSCs, and there were no discernible age-associated changes in MSC marker profiles, consistent with previous reports.[7,18] It should be noted that the isolation of MSCs according to the International Society for Cellular Therapy criteria produces heterogeneous, nonclonal cultures of stromal cells containing stem cells with different multipotential properties, committed progenitors, and differentiated cells.[19] We did not purify the homogenous MSC populations because the presence of different cell types in the SVF might be beneficial in its therapeutic properties.[20]

However, hASCs obtained from aged donors displayed increased senescent features, such as increased SA-β-gal activity, enhanced oxidative damage, and high expression of *p21*. Senescence is considered to be a stress response triggered by the activation of *p53* and is highly influenced by oxidative stress.[21,22] In our study, we observed that hASCs isolated from elder donors expressed higher levels of *p21* mRNA and SA-β-gal activity. *p53* and *p16* were also increased with increasing donor age, although there were no significant differences between groups. These findings are in agreement with existing data, indicating that *p53, p21*, and *p16* lead to cell cycle arrest, senescence, apoptosis, and differentiation, which increase with age.[23] The retinoblastoma family genes *RB1* and *RB2* play a major role in controlling the cell cycle G_1/S transition and regulating some cellular processes, such as terminal differentiation and senescence.[24] Previous studies have shown the switch from *RB1* to *RB2*, including decreased levels of *RB1* and increased levels of *RB2* when cells enter senescent arrest.[25] In hASCs from

different age donors, we observed a decreasing trend in *RB1* mRNA expression with increasing age; however, there was no significant difference across age-groups in *RB1* or *RB2* expression.

The DCFH-DA assay and MitoSOX Red staining demonstrated that intracellular total and mitochondrial-specific ROS production were increased in the elderly group. Obtained data stand in good agreement with Kornicka et al. findings that ROS levels significantly increased with age, being the lowest in the child group, but they maintained on a comparable level in older donors.[26] Another important aspect of cellular senescence is the impaired proteasome activity.[27] An impairment of proteasome activity results in damaged proteins (oxidized, misfolded, and denatured) accumulation, which may induce senescence. In previous studies, proteasome activity is impaired in some forms of senescence: either acute senescence in U937 leukemic cells[28] or chronic replicative senescence in human fibroblasts.[29] The results of our study showed a decreasing trend of proteasome activity in adult donors (young adult group and elderly group) compared to child donors. These data are consistent with the work of Kozil et al., who reported proteasome activity was significantly decreased in fibroblasts from middle-aged donors compared with young donors, and there are a coregulation of mitochondrial and proteasome function.[29] A decrease in *hTERT* and *SIRT1* activity was also detected in the elderly group, while no significant difference in *hTERT* or *SIRT1* mRNA expression was detected between the groups. Telomerase reverse transcriptase is the catalytic subunit of telomerase, which stabilizes telomere length and affects age-relevant processes linked to optimal mitochondrial and stem cell function.[30] Sirt is a family of histone deacetylases that have been shown to regulate the organismal life span, oxidative stress, and DNA damage.[31] Using different model organisms, Sirt1 and Sirt2 have been implicated in life extension.[32]

Our results indicate that hASCs from aged donors undergo a cellular senescence process, although some results did not show a significant difference. Increasing sample sizes for each age range chosen could help describe this relationship more clearly.

Cellular senescence may be ultimately reflected in cell self-renew, proliferation, apoptosis, cell cycle, and differentiation. CFU-F is an important feature of self-renewing stem cells. We observed a significant negative effect of age on hASCs frequency based on the CFU-Fs analysis, in accordance with Kornicka et al, who also observed reduced potential of CFU-Fs forming in older patients.[26] Our results show that age does not significantly affect proliferation and apoptosis. However, a decreasing trend of *c-Jun* and *c-Fos* gene expression, the key proto-oncogenes related to proliferation, with age was observed. Interestingly, our data showed an abnormal cell cycle profile. A significant decrease in the S phase profile in hASCs from the elderly group was found and the expression of *CHEK1*, a cell cycle regulator, displayed a marginal increase in the elderly group compared

with the younger groups. The report of age-associated cell cycle changes in hASCs and BMSCs by Alt et al. support our findings[33]; however, they found the overexpression of *Bcl2* and other genes associated with apoptosis.

Regarding age-related adipogenic differentiation, there are conflicting observations. Despite there being some variations among the 3 groups in terms of the expression levels of the early adipogenic markers (i.e., *PPAR-γ, CEBP-α, FABP4*, adiponectin, and *LPL*), the actual quantity of lipid droplet accumulation present at completion of the experiment was not significantly different. This was confirmed by the expression of lipid synthesis-related genes, such as *GPDH, FASN, ACC1*, and *HSL*. Therefore, hASCs isolated from aged donors had the capacity to retain their overall adipogenic differentiation potential compared to those in the child group. These observations are in line with the work by Choudhery et al.[34] and Zhu et al.,[6] who reported that the adipogenic potential of hASCs was well-preserved in advanced age. However, through more detailed testing, we found a slower response of hASCs to adipogenic inducing factors from the elderly.

Our data signify that aging processes have drastic effects on the osteogenic differentiation potential of hASCs. Quantitative measurement of Alizarin Red S revealed a significant decrease in matrix calcification in the elderly group compared to the child group. Furthermore, differences between groups were observed during both the early and mid-phases of osteogenesis, as determined by the quantitative analysis of molecular markers of osteogenic differentiation. Age-related changes in the osteogenic potential of hASCs were investigated previously in both human and animal studies. For example, consistent with our results, Choudhery et al.[34] showed a significant decrease in osteocalcin and ALP gene expression in elderly donors. However, Weinzierl et al.[35] described no significant age-related changes in the osteogenic potential from hASC donors aged 12 to 75 years. These discrepancies could be due to the different age ranges and health states of the cell donors.

MSCs show great repair capacity, which involves differentiation and migration properties. MSCs can change their membrane receptors and are capable of migration toward the site of the damage.[36] To date, local injection of MSCs is the most prevalent cell delivery method, but inadequate migration limits the therapeutic effect.[37] Current studies are mostly based on the differentiation properties of MSCs, but few have reported the effects of age on migration ability. The results of our study clearly demonstrate a correlation between age and impairment of hASCs migration potential; both the scratch test and the transwell system demonstrated that the migration ability of hASCs in the elderly group was decreased significantly as early as 6 h after culture. The abilities of hASCs to secrete chemokines and express chemokine receptors affect their migration activity. The production of these factors, such as *CXCR4* and *CXCR7*, declines with age, causing impaired hASCs migration potential. Both CXCR4 and CXCR7 are intricately involved in orchestrating the effects of multiple chemokine ligands through distinct signaling mediators to execute differential response and migration of MSCs. Kim et al. reported the overexpression of CXCR4 improved homing and engraftment of hASCs in an animal limb ischemia model.[38] Based on the results presented in our current work, further studies are needed in order to explain the apparent complexities between chemokine receptors and MSC function.

Conclusion

We demonstrated that hASCs from older patients maintained MSC characteristics but acquired some properties of senescent cells. Moreover, aging could affect the differentiation potential of hASCs obtained from older individuals that may restrict the effectiveness of autologous cell therapy with hASCs. In addition, hASCs derived from aged subjects show an impaired migration ability. Therefore, although the different populations were phenotypically similar, they presented major differences at the functional level. In general, hASCs derived from elderly subjects present lower capacity for therapeutic repair.

Further analysis of the function of hASCs in chronologically aged donors is needed to confirm the use of autologous stem cell-based therapeutic strategies.

Ethical Approval

This study was approved by ethics committee of Plastic Surgery Hospital (Institute), Chinese Academy of Medical Sciences and Peking Union Medical College.

Statement of Human and Animal Rights

The ethics committee of Plastic Surgery Hospital (Institute), Chinese Academy of Medical Sciences and Peking Union Medical College approved the use of human-derived tissue samples. Human subcutaneous adipose tissue samples (>5 mL) were excised from the right chest regions of both male and female donors during various surgical procedures following written consent.

Statement of Informed Consent

Written informed consent for the harvest and use of adipose tissue samples for research purposes was obtained from each patient.

Declaration of Conflicting Interests

The author(s) declared no potential conflicts of interest with respect to the research, authorship, and/or publication of this article.

Funding

References

1. Gimble JM, Bunnell BA, Floyd ZE. Prospecting for adipose progenitor cell biomarkers: biopanning for gold with in vivo phage display. Cell Stem Cell. 2011;9(1):1–2.

2. Nicpon J, Marycz K, Grzesiak J. Therapeutic effect of adipose-derived mesenchymal stem cell injection in horses suffering from bone spavin. Pol J Vet Sci. 2013;16(4):753–754.

3. Tzouvelekis A, Paspaliaris V, Koliakos G, Ntolios P, Bouros E, Oikonomou A, Zissimopoulos A, Boussios N, Dardzinski B, Gritzalis D, et al. A prospective, non-randomized, no placebo-controlled, phase Ib clinical trial to study the safety of the adipose derived stromal cells-stromal vascular fraction in idiopathic pulmonary fibrosis. J Transl Med. 2013;11:171.

4. Murohara T, Shintani S, Kondo K. Autologous adipose-derived regenerative cells for therapeutic angiogenesis. Curr Pharm Des. 2009;15(24):2784–2790.

5. Campisi J. Senescent cells, tumor suppression, and organismal aging: good citizens, bad neighbors. Cell. 2005;120(4):513–522.

6. Zhu M, Kohan E, Bradley J, Hedrick M, Benhaim P, Zuk P. The effect of age on osteogenic, adipogenic and proliferative potential of female adipose-derived stem cells. J Tissue Eng Regen Med. 2009;3(4):290–301.

7. Efimenko A, Dzhoyashvili N, Kalinina N, Kochegura T, Akchurin R, Tkachuk V, Parfyonova Y. Adipose-derived mesenchymal stromal cells from aged patients with coronary artery disease keep mesenchymal stromal cell properties but exhibit characteristics of aging and have impaired angiogenic potential. Stem Cells Transl Med. 2014;3(1):32–41.

8. Yang Z, Dong P, Fu X, Li Q, Ma S, Wu D, Kang N, Liu X, Yan L, Xiao R. CD49f Acts as an inflammation sensor to regulate differentiation, adhesion, and migration of human mesenchymal stem cells. Stem Cells. 2015;33(9):2798–2810.

9. Dos-Anjos Vilaboa S, Navarro-Palou M, Llull R. Age influence on stromal vascular fraction cell yield obtained from human lipoaspirates. Cytotherapy. 2014;16(8):1092–1097.

10. Dominici M, Le Blanc K, Mueller I, Slaper-Cortenbach I, Marini F, Krause D, Deans R, Keating A, Prockop D, Horwitz E. Minimal criteria for defining multipotent mesenchymal stromal cells. The international society for cellular therapy position statement. Cytotherapy. 2006;8(4):315–317.

11. Sahin E, Depinho RA. Linking functional decline of telomeres, mitochondria and stem cells during ageing. Nature. 2010;464(7288):520–528.

12. Sethe S, Scutt A, Stolzing A. Aging of mesenchymal stem cells. Ageing Res Rev. 2006;5(1):91–116.

13. Velarde MC, Flynn JM, Day NU, Melov S, Campisi J. Mitochondrial oxidative stress caused by Sod2 deficiency promotes cellular senescence and aging phenotypes in the skin. Aging (Albany NY). 2012;4(1):3–12.

14. Galderisi U, Cipollaro M, Giordano A. The retinoblastoma gene is involved in multiple aspects of stem cell biology. Oncogene. 2006;25(38):5250–5256.

15. Kim M, Kim I, Lee SK, Bang SI, Lim SY. Clinical trial of autologous differentiated adipocytes from stem cells derived from human adipose tissue. Dermatol Surg. 2011;37(6):750–759.

16. Casteilla L, Planat-Benard V, Laharrague P, Cousin B. Adipose-derived stromal cells: their identity and uses in clinical trials, an update. World J Stem Cells. 2011;3(4):25–33.

17. Buschmann J, Gao S, Harter L, Hemmi S, Welti M, Werner CM, Calcagni M, Cinelli P, Wanner GA. Yield and proliferation rate of adipose-derived stromal cells as a function of age, body mass index and harvest site-increasing the yield by use of adherent and supernatant fractions? Cytotherapy. 2013;15(9):1098–1105.

18. Pandey AC, Semon JA, Kaushal D, O'Sullivan RP, Glowacki J, Gimble JM, Bunnell BA. MicroRNA profiling reveals age-dependent differential expression of nuclear factor kappaB and mitogen-activated protein kinase in adipose and bone marrow-derived human mesenchymal stem cells. Stem Cell Res Ther. 2011;2(6):49.

19. Squillaro T, Peluso G, Galderisi U. Clinical trials with mesenchymal stem cells: an update. Cell Transplant. 2016;25(5):829–848.

20. Dykstra JA, Facile T, Patrick RJ, Francis KR, Milanovich S, Weimer JM, Kota DJ. Concise review: fat and furious: harnessing the full potential of adipose-derived stromal vascular fraction. Stem Cells Transl Med. 2017;6(4):1096–1108.

21. Estrada JC, Torres Y, Benguria A, Dopazo A, Roche E, Carrera-Quintanar L, Perez RA, Enriquez JA, Torres R, Ramirez JC, et al. Human mesenchymal stem cell-replicative senescence and oxidative stress are closely linked to aneuploidy. Cell Death Dis. 2013;4:e691.

22. Maredziak M, Marycz K, Tomaszewski KA, Kornicka K, Henry BM. The influence of aging on the regenerative potential of human adipose derived mesenchymal stem cells. Stem Cells Int. 2016;2016:2152435. doi: 10.1155/2016/2152435. Epub ahead of print 2016 Jan 28.

23. Signer RA, Morrison SJ. Mechanisms that regulate stem cell aging and life span. Cell Stem Cell. 2013;12(2):152–165.

24. Alessio N, Bohn W, Rauchberger V, Rizzolio F, Cipollaro M, Rosemann M, Irmler M, Beckers J, Giordano A, Galderisi U. Silencing of RB1 but not of RB2/P130 induces cellular senescence and impairs the differentiation potential of human mesenchymal stem cells. Cell Mol Life Sci. 2013;70(9):1637–1651.

25. Helmbold H, Galderisi U, Bohn W. The switch from pRb/p105 to Rb2/p130 in DNA damage and cellular senescence. J Cell Physiol. 2012;227(2):508–513.

26. Kornicka K, Marycz K, Tomaszewski KA, Maredziak M, Smieszek A. The effect of age on osteogenic and adipogenic differentiation potential of human adipose derived stromal stem cells (hASCs) and the impact of stress factors in the course of the differentiation process. Oxid Med Cell Longev. 2015;2015:309169. doi: 10.1155/2015/309169. Epub ahead of print 2015 Jul 12.

27. Capasso S, Alessio N, Squillaro T, Di Bernardo G, Melone MA, Cipollaro M, Peluso G, Galderisi U. Changes in autophagy, proteasome activity and metabolism to determine a specific signature for acute and chronic senescent mesenchymal stromal cells. Oncotarget. 2015;6(37):39457–39468.

28. Bertram C, Hass R. Matrix metalloproteinase-7 and the 20S proteasome contribute to cellular senescence. Sci Signal. 2008; 1(12):pt1.

29. Koziel R, Greussing R, Maier AB, Declercq L, Jansen-Durr P. Functional interplay between mitochondrial and proteasome activity in skin aging. J Invest Dermatol. 2011;131(3):594–603.

30. Sarin KY, Cheung P, Gilison D, Lee E, Tennen RI, Wang E, Artandi MK, Oro AE, Artandi SE. Conditional telomerase induction causes proliferation of hair follicle stem cells. Nature. 2005;436(7053):1048–1052.

31. Mostoslavsky R, Chua KF, Lombard DB, Pang WW, Fischer MR, Gellon L, Liu P, Mostoslavsky G, Franco S, Murphy MM, et al. Genomic instability and aging-like phenotype in the absence of mammalian SIRT6. Cell. 2006;124(2):315–329.

32. Kaeberlein M, McVey M, Guarente L. The SIR2/3/4 complex and SIR2 alone promote longevity in Saccharomyces cerevisiae by two different mechanisms. Genes Dev. 1999; 13(19):2570–2580.

33. Alt EU, Senst C, Murthy SN, Slakey DP, Dupin CL, Chaffin AE, Kadowitz PJ, Izadpanah R. Aging alters tissue resident mesenchymal stem cell properties. Stem Cell Res. 2012;8(2): 215–225.

34. Choudhery MS, Badowski M, Muise A, Pierce J, Harris DT. Donor age negatively impacts adipose tissue-derived mesenchymal stem cell expansion and differentiation. J Transl Med. 2014;12:8. doi: 10.1186/1479-5876-12-8.

35. Weinzierl K, Hemprich A, Frerich B. Bone engineering with adipose tissue derived stromal cells. J Craniomaxillofac Surg. 2006;34(8):466–471.

36. Annabi B, Lee YT, Turcotte S, Naud E, Desrosiers RR, Champagne M, Eliopoulos N, Galipeau J, Beliveau R. Hypoxia promotes murine bone-marrow-derived stromal cell migration and tube formation. Stem Cells. 2003;21(3):337–347.

37. Habisch HJ, Janowski M, Binder D, Kuzma-Kozakiewicz M, Widmann A, Habich A, Schwalenstocker B, Hermann A, Brenner R, Lukomska B, et al. Intrathecal application of neuroectodermally converted stem cells into a mouse model of ALS: limited intraparenchymal migration and survival narrows therapeutic effects. J Neural Transm (Vienna). 2007;114(11): 1395–1406.

38. Kim M, Kim DI, Kim EK, Kim CW. CXCR4 overexpression in human adipose tissue-dervied stem cells improves homing and engraftment in an animal limb ischemia model. Cell Transplant. 2017; 26(2): 191–204.